

Article

An Ab Initio Investigation of the Hydration of Antimony(III)

Cory C. Pye *  and Champika Mahesh Gunasekara

Department of Chemistry, Saint Mary's University, Halifax, NS B3H 3C3, Canada

* Correspondence: cory.pye@smu.ca

Abstract: The energies, structures, and vibrational frequencies of $[\text{Sb}(\text{H}_2\text{O})_n]^{3+}$, $n = 0-9$, 18 have been calculated at the Hartree–Fock and second-order Møller–Plesset levels of theory using the CEP, LANL2, and SDD effective core potentials in combination with their associated basis sets, or with the 6-31G* and 6-31+G* basis sets. The metal–oxygen distances and totally symmetric stretching frequency of the aqua ions were compared with each other and with related crystal structure measurements where available.

Keywords: ab initio; antimony(III); hydration; symmetry; vibrational spectrum

1. Introduction

Although the structure of many metal ions in solution is known, some remain elusive [1]. Many are known to be toxic to man, but this is dependent on the oxidation state and speciation, which often depends on pH and the presence of counterions that solubilize the metal by complex formation. While computational chemistry can assist in supporting and rationalizing proposed speciation models, one drawback is that there are typically few all-electron basis sets that can be used. For elements with a high atomic number, relativistic effects can play an important role. Effective core potentials (ECPs) replace the explicit description of core electrons by a potential, and are paired with basis sets describing the outermost electrons. The ECPs represent the scalar relativistic effects only, but the spin–orbital relativistic effects should be small. In a previous work, we benchmarked some common ECPs for the aqua complexes of the heavy metals mercury(II) and thallium(III), both of which have valence electron configuration $5d^{10}$ [2]. It was shown that the ECPs reproduce the known hexacoordination of thallium(III), and supported a hexacoordinate model for mercury(II) over a heptacoordinate model. We also extended this work to lead(II), with valence electron configuration $6s^2 5d^{10}$ [3]. The presence of an ns^2 subshell can give rise to either *hemidirected* structures (which tend to be favored at lower coordination numbers) with ligands that are not symmetrically distributed around the central ion, or *holodirected* structures with a symmetrical distribution. No consensus exists on the coordination number of lead(II), with predictions ranging from 4 to 9, but our results were most consistent with a hemidirected hexaaqualead(II) species. For the smaller aquatin(II) ion ($5s^2 4d^{10}$), we found that the preferred hydration mode was a tricoordinate trigonal pyramidal triaquatin(II), agreeing with recent experiments [4]. We extend our work now to antimony(III), which has the same valence electron configuration as tin(II) but a higher charge. The structure of aquaantimony(III) is unknown, so one of our aims is to predict its structure. The presence of the ns^2 subshell, as with lead(II) and tin(II), will be shown to have a pronounced effect on the structures compared to those without it.

The literature on the solution chemistry of antimony(III) is sparse. The solubility of rhombic Sb_2O_3 was examined by Gayer and Garrett over half a century ago, and they proposed that dissolved antimony(III) exists as SbO^+ , $\text{Sb}(\text{OH})_3$, and SbO_2^- as the pH is increased [5]. This was confirmed spectrophotometrically by Mishra and Gupta, who suggested that the neutral species could be either $\text{Sb}(\text{OH})_3$ or $\text{SbO}(\text{OH})$ [6]. Potentiometrically, SbO^+ is equivalent to $\text{Sb}(\text{OH})_2^+$, SbO_2^- is equivalent to $\text{Sb}(\text{OH})_4^-$, and Sb^{3+} is proposed



Citation: Pye, C.C.; Gunasekara, C.M. An Ab Initio Investigation of the Hydration of Antimony(III). *Liquids* **2024**, *4*, 322–331. <https://doi.org/10.3390/liquids4020016>

Academic Editor: Enrico Bodo

Received: 4 November 2023

Revised: 2 February 2024

Accepted: 5 March 2024

Published: 1 April 2024



Copyright: © 2024 by the authors. Licensee MDPI, Basel, Switzerland. This article is an open access article distributed under the terms and conditions of the Creative Commons Attribution (CC BY) license (<https://creativecommons.org/licenses/by/4.0/>).

to exist only in strongly acidic solutions [7]. Ahrlund and Bovin examined the solution chemistry of antimony(III) oxide in perchloric and nitric acid [8]. At an ionic strength of 5.0 mol/L, maintained by sodium perchlorate or nitrate, the two modifications of $\text{Sb}_2\text{O}_3(\text{s})$ are only metastable above a perchloric acid concentration of 0.3 mol/L (orthorhombic) or 0.7 mol/L (cubic), and the equilibrium solid phase is $\text{Sb}_4\text{O}_5(\text{OH})\text{ClO}_4 \cdot 1/2\text{H}_2\text{O}$. Other solid phases exist at higher acid concentrations. In nitric acid at a nitrate concentration of 5.0 mol/L, the equilibrium solid phase is $\text{Sb}_4\text{O}_4(\text{OH})_2(\text{NO}_3)_2$. Analysis suggests that the aqueous speciation at a low pH consists of $\text{Sb}(\text{OH})_2^+$, and possibly $\text{Sb}_2(\text{OH})_2^{4+}$. Zakaznova-Herzog and Seward used UV/visible spectroscopy to examine the equilibria of antimonous acid and was able to explain their results using the species $\text{H}_3\text{SbO}_3(\text{aq})$, H_4SbO_3^+ , and $\text{H}_2\text{SbO}_3^-(\text{aq})$ from 25–300 °C, pH = 0.8–12.5 at a total antimony concentration of $\sim 10^{-4}$ mol/L [9].

We now consider if insight may be gained by examining the solid-state structures of antimony oxides and their hydrates. Antimony(V) oxide, and its mono and trihydrate, were discussed by Natta and Baccaredda [10]. Well-aged (5 years!) monohydrate $\text{Sb}_2\text{O}_5 \cdot \text{H}_2\text{O}$ (also known as antimonic acid, HSbO_3) was found to belong to a cubic space group (Schönflies notation, O_h^7 ; Hermann–Mauguin notation, $Fd\bar{3}m_2$), with $a = 10.23 \pm 0.02$ Å, $Z = 8$. The compound Sb_2O_4 of the same space group was formulated as the pyroantimonate $[\text{Sb}^{\text{III}}_2\text{O}]^{4+}[\text{Sb}^{\text{V}}_2\text{O}_7]^{4-}$. However, Dihlstrom and Westgren suggested that “ Sb_2O_4 ” was actually $\text{Sb}_3\text{O}_6\text{OH}$, as $\text{Sb}^{\text{III}}\text{OOH} \cdot \text{Sb}^{\text{V}}_2\text{O}_5$, with $a = 10.28$ Å [11]. They found the distances Sb^{III}-O, 2.48 Å; Sb^{III}-O(H), 2.23 Å, Sb^V-O, 2.02 Å. Another form of antimonic acid, $\text{Sb}_2\text{O}_5 \cdot 3\text{H}_2\text{O}$, was found by England et al. to have a pyrochlore ($\text{A}_2\text{M}_2\text{O}_6\text{O}'$, $Fd\bar{3}m$) structure via powder diffraction [12]. Other forms, described by Watelet et al. as $[\text{H}(\text{H}_2\text{O})_n]_{12}\text{Sb}_{12}\text{O}_{36}$, ($n = 0.33, 1$), space group $Im\bar{3}$, $a = 9.470(5)$, and $9.497(3)$ Å, respectively, have Sb-O distances in the range 1.939–2.006 Å [13]. These solids are proton conductors. Another antimony oxide hydroxide HSb_3O_8 was described by Jager et al. [14] as space group $P2_1/n$, with cell constants $a = 9.456(2)$, $b = 8.691(2)$, $c = 9.909(2)$ Å, $\beta = 90.25(2)^\circ$, $Z = 6$. The Sb-O distances fall in the range 1.890–2.140 Å. Riviere et al. obtained an $Fd\bar{3}m$ space group for $\text{H}_2\text{Sb}_2\text{O}_6 \cdot \text{H}_2\text{O}$, $a = 10.365(2)$ Å, with Sb-O = 1.971 Å [15]. For antimony(III) oxide, the structure of the cubic α form was refined by Svensson [16], who found a space group $Fd\bar{3}m$ and $a = 11.1519(2)$ Å. It forms discrete Sb_4O_6 units of symmetry T_d with trigonal pyramidal antimony(III) with an Sb-O distance of 1.977(1) Å and angles of $95.93(8)^\circ$. Svensson also examined the orthorhombic β modification of antimony(III) oxide [17], and found a space group $Pccn$, $a = 4.911$, $b = 12.464$, $c = 5.412$ Å. The structure is composed of double infinite chains, with the antimony lone pair perpendicular to the chains. The antimony is trigonal pyramidal, with Sb-O distances in the range 1.977(7)–2.023(4) Å. A novel γ modification was reported by Orosel et al., with space group $P2_12_12_1$, $a = 11.6411(1)$, $b = 7.5666(0)$, $c = 7.4771(0)$ Å, with Sb-O distances in the range 1.87–2.24 Å [18]. In $\text{Sb}_4\text{O}_4(\text{OH})_2(\text{NO}_3)_2$, Bovin found sheets of 3-coordinate trigonal pyramidal and 4-coordinate seesaw antimony(III) separated by nitrate ions [19]. The Sb-O distances in the SbO_3 units are in the range 1.942(7)–2.067(6) Å, and in the SbO_4 units, 2.019(6)–2.265(6) Å. In $\text{Sb}_4\text{O}_5(\text{OH})\text{ClO}_4 \cdot 1/2\text{H}_2\text{O}$, Bovin found short chains of SbO_n polyhedra forming layers separated by the perchlorate ions and water molecules [20]. The Sb-O distances in the SbO_3 units are in the range 1.969(11)–2.027(8) Å, and in the SbO_4 units, 1.952(9)–2.378(8) Å. In the antimony oxide sulfate $\text{Sb}_6\text{O}_7(\text{SO}_4)_2$, Bovin found that the three unique antimony atoms were trigonally pyramidally coordinated to oxygen atoms, with Sb-O distances between 1.994(17) and 2.207(18) Å, but with a fourth oxygen close 2.327(14)–2.382(18) [21]. Mercier et al. found for the oxonium antimony sulfate, $(\text{H}_3\text{O})_2\text{Sb}_2(\text{SO}_4)_4$, that antimony exists as both a seesaw SbO_4 and square pyramidal SbO_5 polyhedra, with corresponding distances of 2.032(10)–2.359(19) Å and 2.012(15)–2.263(13) Å [22]. The axial distance of SbO_5 is the shortest. To summarize this literature, antimony(V) tends to exist as an octahedrally coordinated moiety in the presence of oxide/hydroxide, whereas antimony(III) can exist as either a trigonal pyramidal SbO_3 , seesaw SbO_4 , or square pyramidal SbO_5 coordinated moiety in a similar environment.

2. Materials and Methods

Calculations were performed using Gaussian 98 [23]. In this program version, the ability to calculate analytical frequencies of molecules in which core electrons are described by effective core potentials was introduced. Therefore, many variants of these were tried. The MP2 calculations use the frozen core approximation. A stepping-stone approach was used for geometry optimization, in which the geometries at the levels HF/CEP-4G, HF/CEP-31G*, HF/CEP-121G*, HF/LANL2MB, HF/LANL2DZ, and HF/SDD were sequentially optimized. For minimum energy structures, the MP2/CEP-31G* and MP2/CEP-121G* calculations were also performed. Calculations were also carried out using the 6-31G* and 6-31+G* basis sets on the atoms of the water molecules (5d) with an effective core potential and basis set on the metal ion (denoted as ECP+6-31G* or 6-31+G*). For shorthand, we denote the mixed basis sets as follows: CEP-121G* on Sb, 6-31G* on O,H, as basis set A; LANL2DZ on Sb, 6-31G* on O, H, as basis set B; SDD on Sb, 6-31G* on O,H, as basis set C; and the corresponding basis sets with diffuse functions are indicated by adding a “+” to the basis set name. Default optimization specifications were used. After each level, where possible, a frequency calculation was performed at the same level and the resulting Hessian was used in the following optimization. Z-matrix coordinates constrained to the appropriate symmetry were used to speed up the optimizations. Because frequency calculations are carried out at each level, any problems with the Z-matrix coordinates would manifest themselves by giving imaginary frequencies corresponding to modes orthogonal to the spanned Z-matrix space. The Hessian was evaluated at the first geometry (opt = CalcFC) for the first level in a series to aid geometry convergence. We note that, for the heavy elements only, the three different CEP basis sets are equivalent (CEP-121G*) but differ for the oxygen and hydrogen atoms. The choice of core electrons defining the pseudopotential depends on the specific core potential (CEP and LANL2, [Kr]4d¹⁰; SDD, [Ar]3d¹⁰). Gaussian 03 [24] and Gaussian 16 [25] were used to correct errors and omissions.

In many cases to follow, the symmetry of the minimum energy complexes was the same as those previously found for bismuth [26]. To confirm these results, starting with high symmetry structures, systematic desymmetrization along the various irreducible representations was carried out [27,28]. We did not employ an implicit solvation model for reasons described previously [3].

3. Results

3.1. A Survey of Structures

Antimony(III) might be expected to show similar properties to tin(II), although the higher charge would cause stronger interactions with water molecules. The point group symmetry for mono- through octaquaantimony(III) was initially usually found to be C_{2v} , C_2 , C_3 , C_{2v} or C_2 , C_{2v} , C_3 , C_{2v} [5+2], and S_8 , respectively. The diaquaantimony(III) species, like lead and tin, ascended in symmetry to a planar C_{2v} structure at HF/LANL2MB. Initially, all attempts to generate a stable 7-coordinate antimony resulted in two water molecules moving to the second hydration sphere. We initially did not find a stable D_3 enneaquaantimony(III) structure.

The results of the systematic desymmetrization procedure [27] for aquaantimony(III) are as follows (see Figures 1 and S1):

- The monoquaantimony(III) remains C_{2v} at all levels.
- The most stable diaquaantimony(III) remains the bent C_2 at all levels except HF/LANL2MB (C_{2v} planar). The linear holodirected D_{2d} structure is approximately 50 kJ/mol higher in energy, but the unstable bent C_s structure is only slightly higher in energy (<1 kJ/mol for nonminimal basis sets). All attempts to generate a [1+1] structure instead result either in proton transfer to give $SbOH^{2+} + H_3O^+$, which was much lower in energy, or recoordination to give the [2+0] C_s structure.
- The most stable triquaantimony(III) remains the pyramidal C_3 at all levels. The two pyramidal C_{3v} structures are 10–30 kJ/mol higher in energy, whereas the planar holodirected D_{3h} and D_3 structures are 125–150 kJ/mol higher in energy still. The unstable

- [2+1] C_{2v} structure was ~ 90 kJ/mol higher in energy, and upon desymmetrization, underwent proton transfer to give the much-lower-in-energy $\text{SbOH}(\text{H}_2\text{O})_2^{2+} + \text{H}_3\text{O}^+$.
- The most stable tetraaquaantimony(III) is usually the seesaw C_{2v} #3 (all mixed basis sets, HF/SDD), but it can be C_2 (all CEP, HF/LANL2DZ) or C_s (HF/LANL2MB). The other C_{2v} structures are higher in energy (10–25 kJ/mol). The holodirected D_{2d} #1, #2, and S_4 structures are much higher in energy (75–125 kJ/mol). The unstable C_s #2 [3+1] structures are up to 50 kJ/mol higher in energy, and upon desymmetrization, undergo a proton transfer to give the much-lower-in-energy $\text{SbOH}(\text{H}_2\text{O})_2^{2+} + \text{H}_3\text{O}^+$.
 - The most stable pentaquaantimony(III) is the square pyramidal C_{2v} #1, with the other three C_{2v} structures which are 25–50 kJ/mol higher in energy. The usually unstable [4+1] structures are 15–50 kJ/mol higher in energy. To our surprise, the C_{2v} #1 [4+1] is stable at HF/CEP-121G*, HF/LANL2MB, HF/A, HF/B, HF/C, and HF/A+. At the other levels, there is a B_1 imaginary mode, along which a proton transfer occurs to give $\text{SbOH}(\text{H}_2\text{O})_3^{2+} + \text{H}_3\text{O}^+$. At the MP2 levels, desymmetrization along an A_2 mode gives rise to a C_2 structure, which is slightly lower in energy.
 - The most stable hexaquaantimony(III) is the distorted octahedral C_3 . The octahedral T_h structure is ~ 18 –50 kJ/mol higher in energy. The two C_s [5+1] structures examined often underwent proton transfer to give $\text{SbOH}(\text{H}_2\text{O})_4^{2+} + \text{H}_3\text{O}^+$. However, if the [5+1] structures were stationary points, they were lower in energy than the [6+0] forms by about 25 kJ/mol. In some cases, they were actually minima (HF/CEP-121G*, all HF mixed basis sets). Given how shallow (or in some cases, nonexistent) the barrier to proton transfer is to give the deprotonated forms, it is reasonable to conclude that the aquaantimony(III) species would only exist in an extremely acidic solution. Combined with the results for the pentaquaantimony(III), this suggests that antimony(III) is actually pentacoordinate square pyramidal.
 - Of the 16 different C_{2v} heptaquaantimony(III) structures tried, none were stable, either possessing imaginary modes or dissociating to a [6+1], [5+2], or [4+3] structure. Structures #1, #2, and #4, nearly always dissociated. The remainder usually remained 7-coordinate, except occasionally dissociating at HF/CEP-4G and HF/LANL2MB. In some cases, the [5+2] structures underwent a double proton transfer and possibly a water elimination to give $\text{Sb}(\text{OH})_2(\text{H}_2\text{O})_2/3^+ + 1/0\text{H}_2\text{O} + 2\text{H}_3\text{O}^+$. Of the 7-coordinate C_{2v} structures, #16 was the lowest in energy, unless #1 was a stationary point, in which case, it was lower in energy. In all cases, the [5+2] structure was 20–80 kJ/mol lower in energy than the 7-coordinate C_{2v} #16 structure. Upon desymmetrization of the remaining 7-coordinate C_{2v} structures to C_2 , many coalesced to C_2 #16, some dissociated to [5+2], but at some levels, C_2 #5, #6, #11, and #13 also exist, with at least one imaginary B mode. When these were desymmetrized to C_1 #1–5, a stable C_1 #3 or #5 was found at some levels, or ligand dissociation to a [6+1] or [5+2] structure took place. Desymmetrization of the C_{2v} structures along the B modes gave one of 27 possible C_s structures. Of these, C_s #1, #5, and either #13 or #20 often coalesce (to C_s #5); C_s #2, #7, #14 and #22 often coalesce (to C_s #7); C_s #12 coalesces to C_s #8; C_s #11, #18, and #26 often coalesce (to C_s #26); C_s #19 and C_s #15 ascend in symmetry to either C_{2v} #10 or #12; C_s #16 and #24 often coalesce to C_s #10 or to each other; C_s #25 coalesces to C_s #21; C_s #27 coalesces to C_s #23; and C_s #17 remains unique. None of these C_s structures are minima, except C_s #13 at HF/A+. The C_s structures desymmetrize to C_1 #6–21. Of these possibilities, for the most part, they coalesced to the previously found C_1 #3 or #5 structures, or underwent ligand dissociation to give [6+1] or [5+2] structures. This exemplifies the power of the systematic desymmetrization procedure in finding minimum energy structures that would otherwise be difficult to locate. In all cases where a seven-coordinate minimum energy structure exists (HF/CEP-31G*, HF/CEP-121G*, MP2/CEP-31G*, MP2/CEP-121G*, HF/C, HF/A+, HF/B+, HF/C+, MP2/A+), it is less stable than a [5+2] or [6+1] structure (or a proton transferred version thereof). The 7-coordinate structures are unlikely to have any significant population in an aqueous solution under ambient conditions.

- For octaaquaantimony(III), two D_{4h} (square prism) and two D_{4d} (square antiprism) structures were first examined. Multiple imaginary modes were present.
- For the D_{4d} #1 and #2 structures, desymmetrization along the A_2 imaginary mode gave the same S_8 #1 structure; along the B_1 imaginary mode, the same D_4 #2 structure; and along the B_2 imaginary mode, the C_{4v} #1 and #2 structures. For the D_{4h} #1 and #2 structures, desymmetrization along the A_{1u} imaginary mode gave the D_4 #2 structure found before; along the A_{2g} imaginary mode, the same C_{4h} #1 structure; along the A_{2u} imaginary mode, the C_{4v} #3 [4+4] and #4 structures; along the B_{2g} imaginary mode (D_{4h} #1), the D_{2h} #1 structure ascended in symmetry to D_{4h} #2; along the B_{1u} mode, D_{2d} #1 and #3 coalesced; along the B_{2u} mode, D_{2d} #2 and #4, respectively. Another D_{2d} structure (#5) was formed by combining other D_{2d} structures.
- Desymmetrization of the C_{4h} #1 structure along the A_u mode usually gives the S_8 #1 structure (via C_4 #1), and along the B_u mode, D_{2d} #5 (via S_4 #1); the S_8 #1 structure along the B mode at two levels, C_4 #1; the D_4 #1 structure along the A_2 mode, C_4 #1, and along the B_2 mode, D_2 #1; the D_{2d} #1 structure along the A_2 mode, S_4 #2, the B_1 mode, D_2 #1, and the B_2 mode, [4+4] C_{2v} #1; the D_{2d} #2 structure along the A_2 mode, S_4 #2, the B_1 mode, D_2 #1, and the B_2 mode, C_{2v} #2; the D_{2d} #4 structure along the A_2 mode, S_4 #2, the B_1 mode, D_2 #1, and the B_2 mode, C_{2v} #3; the D_{2d} #5 structure along the B_1 mode, D_2 #1, and the B_2 mode, [6+2] C_{2v} #4. All of these structures had at least one imaginary frequency.
- Desymmetrization of the S_4 #2 structure along the B mode, C_2 #1 (which was close in structure to the D_2 #1 structure); the D_2 #1 structure along the B_1 mode gave either the [4+4] or [6+2] C_2 #1, or more usually the stable S_8 #1.
- For enneaquaantimony(III), four D_{3h} structures were first examined. Desymmetrization along the A_1'' mode led to the common D_3 #1 structure (which was only stable at MP2/CEP-31G*); the A_2' mode led to either the unstable C_{3h} #1 or #2 structures; and the A_2'' mode led to the unstable C_{3v} #1–4 structures. The C_{3v} #2 and 3 structures were usually of [6+3] coordination. When these structures were desymmetrized, they nearly always resulted in expulsion of three water molecules to the second hydration sphere to give the (usually) stable C_3 #1 [6+3]. An unstable [6+3] D_3 structure was also found, which desymmetrized to give the even more stable C_3 #2 [6+3].

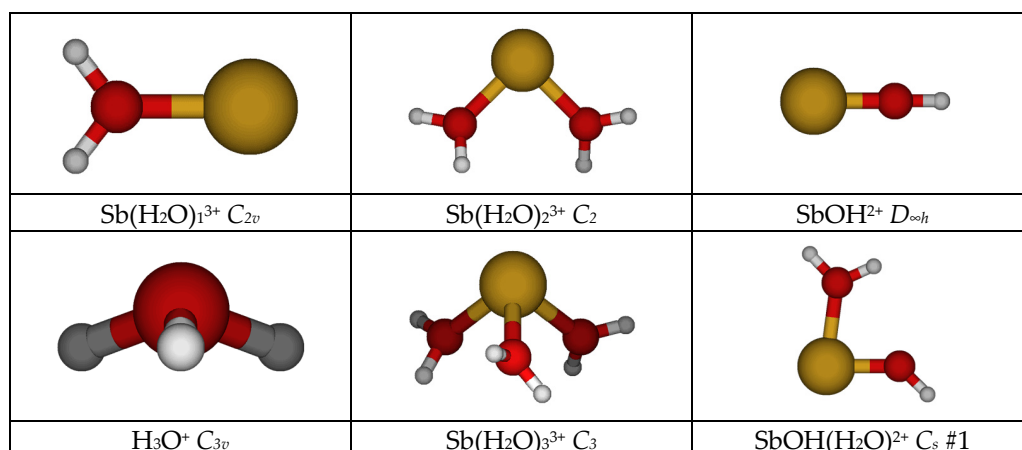


Figure 1. Cont.

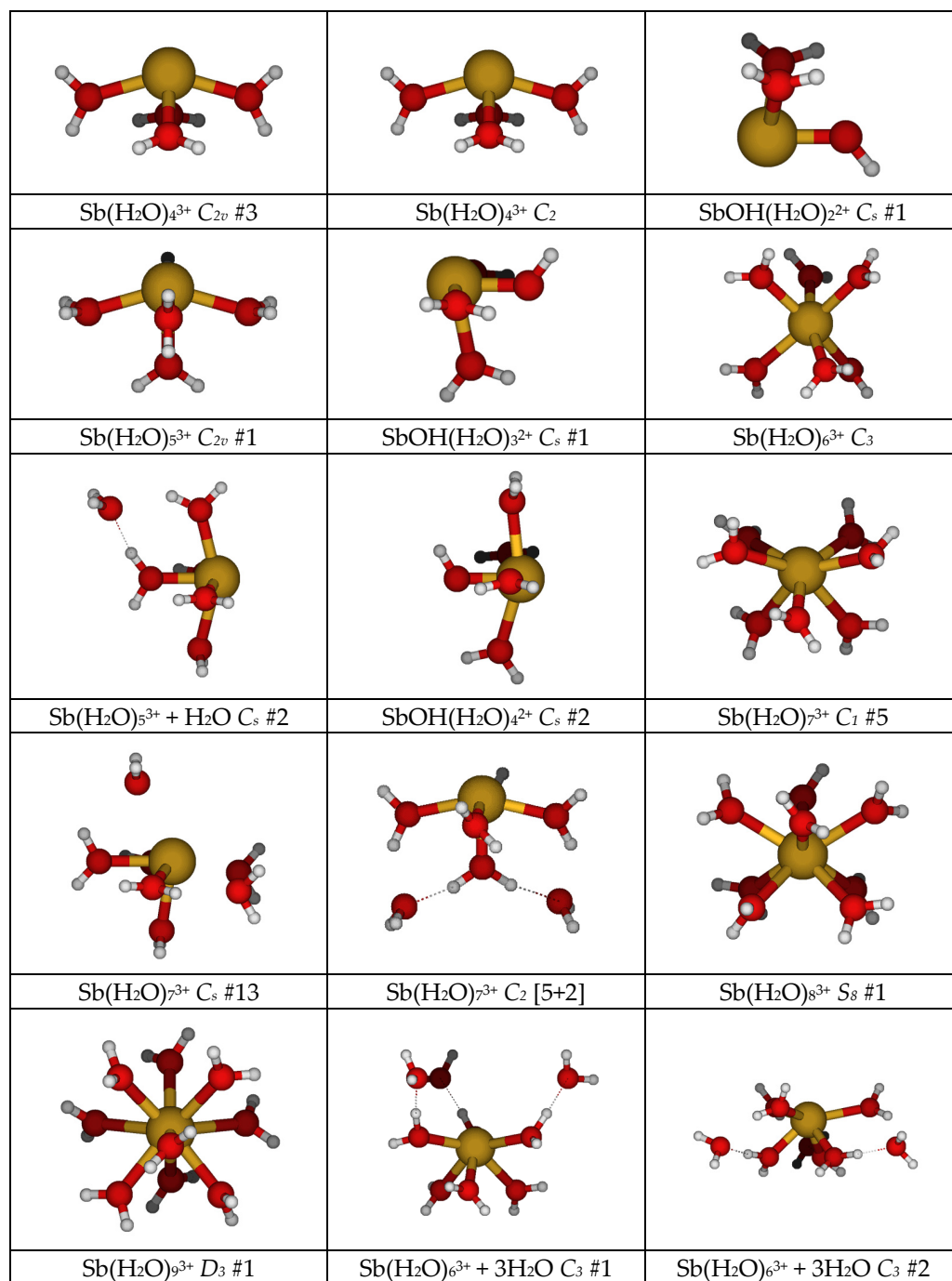


Figure 1. The minimum energy structures of aquaantimony(III) and related species.

To summarize these results, it appears that the square pyramidal pentaquaantimony(III) ion is the most stable aqua ion. There is a strong propensity to react with second-shell water molecules to form hydroxo complexes. While stable structures with coordination numbers between six and nine do exist at some levels of theory, the corresponding structures in which some waters have moved to the second hydration shell are more stable (in some cases, with proton transfer). These higher-coordination aqua complexes might exist at high pressures. The aqua ion, if it exists, would only exist at a very low pH.

3.2. The Sb-O Distance

In Figure 2, a plot of the dependence of the average Sb-O distance as a function of the coordination number n is given for all of the levels investigated. The Sb-O distance lengthened with the increase in coordination number. With the exception of HF/LANL2MB, the results were fairly uniform (for the most part, within 0.05 Å). The HF/LANL2MB level is the only Hartree–Fock level calculation using a minimal basis set on the valence shell of all atoms, and therefore does not have enough flexibility to fully describe the bonding between antimony(III) and oxygen. The pairs HF/CEP-31G* and HF/CEP-121G*, and MP2/CEP-31G* and MP2/CEP-121G*, were nearly coincident with each other, with the latter pair giving slightly longer bond lengths. The variation in the Sb-O distance with the level of theory was smaller than that of Sn-O [4]. Based on our calculations, if the coordination number is indeed 5, then we would expect an average Sb-O distance of around 2.25 Å.

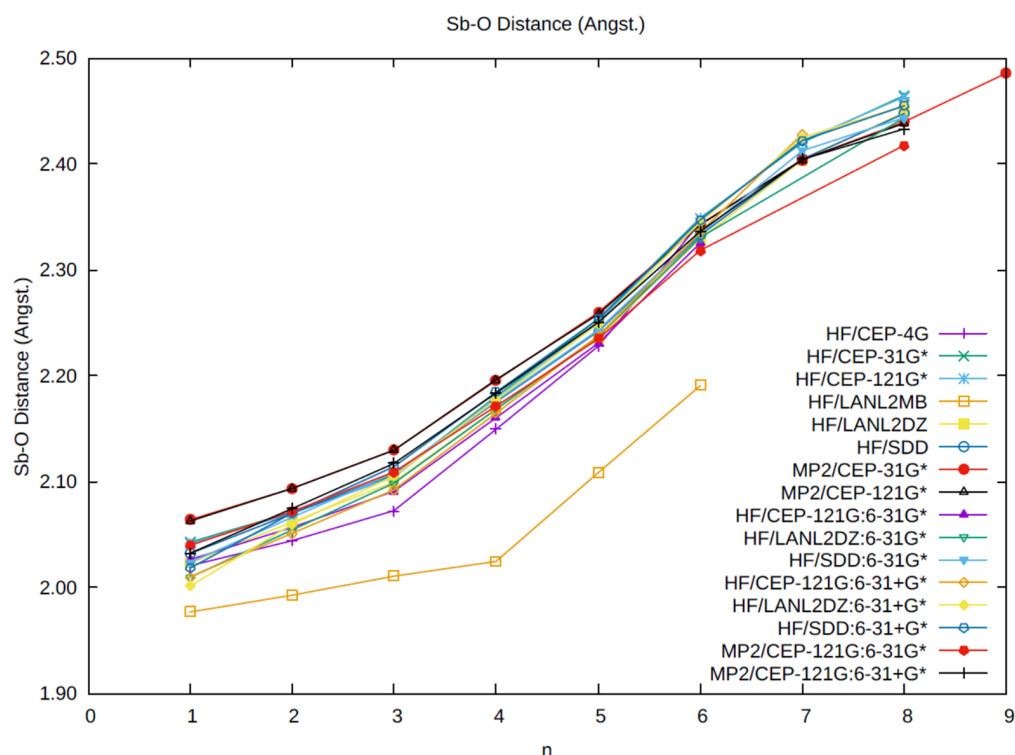


Figure 2. The dependence of the average Sb-O distance (Å) in $\text{Sb}(\text{H}_2\text{O})_n^{3+}$ on the coordination number n and level of theory.

3.3. The Sb-O Vibrational Frequency

In Figure 3, a plot of the dependence of the frequency of the most intense Raman Sb-O stretching mode as a function of the coordination number n is given for all of the levels investigated. As expected, this frequency drops with hydration number n . The minimal basis set levels HF/LANL2MB, and to some extent, HF/CEP-4G, are different than the others, having higher values. The CEP-4G basis set is a minimal basis set on oxygen and hydrogen, but is actually using the triple-zeta valence basis set (CEP-121G) on the antimony atom. There is a levelling off of the frequency, and then a bigger drop at $n = 6$. For $n = 4$ and 5, the vibrational mode is somewhat more localized, being due predominantly to either the equatorial oxygen motion ($n = 4$) or the apical oxygen motion ($n = 5$). The HF/CEP-31G*, HF/CEP-121G*, MP2/CEP-31G*, MP2/CEP-121G*, and MP2/A+ levels form the group with the lowest vibrational frequencies. The HF calculations using the SDD basis set on Sb form a group with the highest vibrational frequencies. For the levels using split valence basis sets, if the coordination number is indeed 5, then the predictions for the Sb-O symmetric stretching motion center around $450 \pm 30 \text{ cm}^{-1}$. In solution, the effect of

the second hydration shell would increase this by an estimated 60 cm^{-1} , meaning that our best guess for the Sb-O mode in an aqueous solution would be 510 cm^{-1} .

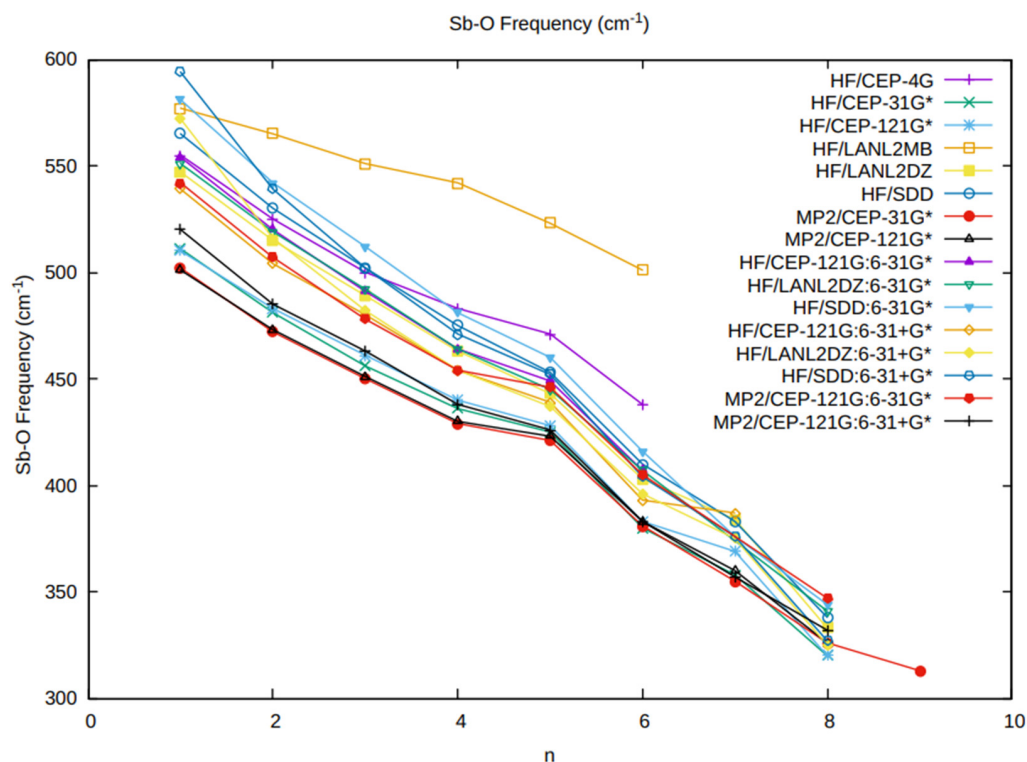


Figure 3. The dependence of the most intense Raman Sb-O frequency (cm^{-1}) in $\text{Sb}(\text{H}_2\text{O})_n^{3+}$ on the coordination number n and level of theory.

4. Discussion

To the best of our knowledge, experimental data on the structure and vibrational spectra of antimony(III) aqua complexes are lacking. Our energetic comparisons suggest that the coordination number should be 5. From this, we have made predictions as to the Sb-O distance ($2.25 \pm 0.05 \text{ \AA}$) and vibrational frequency ($510 \pm 30 \text{ cm}^{-1}$) that might be observed. We may compare the X-ray crystal structures involving $\text{Sb}^{3+}\text{-O}^{2-}$ (or OH^-) interactions with the same coordination geometry. Our predictions for trigonal pyramidal ($n = 3$) lie at around 2.10 \AA (cf. 1.977 \AA in $\alpha\text{-As}_4\text{O}_6$ [16], $1.977\text{--}2.023 \text{ \AA}$ in $\beta\text{-As}_4\text{O}_6$ [16], $1.942\text{--}2.067 \text{ \AA}$ in $\text{Sb}_4\text{O}_4(\text{OH})_2(\text{NO}_3)_2$ [19], $1.969\text{--}2.027 \text{ \AA}$ in $\text{Sb}_4\text{O}_5(\text{OH})\text{ClO}_4 \cdot 1/2\text{H}_2\text{O}$ [20], $1.994\text{--}2.207 \text{ \AA}$ in $\text{Sb}_6\text{O}_7(\text{SO}_4)_2$ [21]); for seesaw ($n = 4$), at around 2.17 \AA (cf. $2.019\text{--}2.265 \text{ \AA}$ in $\text{Sb}_4\text{O}_4(\text{OH})_2(\text{NO}_3)_2$ [19], $1.952\text{--}2.378 \text{ \AA}$ in $\text{Sb}_4\text{O}_5(\text{OH})\text{ClO}_4 \cdot 1/2\text{H}_2\text{O}$ [20], $2.032\text{--}2.359 \text{ \AA}$ in $(\text{H}_3\text{O})_2\text{Sb}_2(\text{SO}_4)_4$ [22]); and for square pyramidal ($n = 5$), at around 2.25 \AA (cf. $2.012\text{--}2.263 \text{ \AA}$ in $(\text{H}_3\text{O})_2\text{Sb}_2(\text{SO}_4)_4$ [22]). The separation by distance between the axial and equatorial sites in the seesaw and square pyramid is reproduced. Our predictions for the $\text{Sb}^{3+}\text{-OH}_2$ distances are about 0.1 \AA longer than the Sb-O distances between the antimony(III) and either the O^{2-} or OH^- moieties in the crystal structures, in which there should be stronger attractive forces.

5. Conclusions

The common CEP, LANL2, and SDD pseudopotentials were paired with various basis sets to study the hydrated antimony(III) ion. Calculations using minimal basis sets (HF/LANL2MB, HF/CEP-4G) performed poorly. The calculated structures of the aqua complexes compared favorably with the crystal structures of the oxides/hydroxides. Symmetry can be used to guide the search for new structures and to rule out structures. For the smaller coordination numbers, the effect of the ns^2 subshell is clearly to form a hemidirected structure in which the electrons act similarly as a ligand or lone pair would.

The factors giving rise to either holodirected or hemidirected structures were thoroughly discussed by Shimony-Livny et al. for Pb(II) and do not need to be repeated here [29]. There is a propensity for the aqua complexes of smaller coordination numbers of type $[n + 1]$ to hydrolyze to form the aquahydroxoantimony(III) complex and a hydronium ion, which is evidence for the strong Lewis acidity of antimony(III). We predict that antimony(III) might exist in extremely acidic solutions with a coordination number of 5, an average Sb-O distance of 2.25 Å, and with a Raman-active Sb-O totally symmetric stretching motion occurring at around 510 cm^{-1} .

Supplementary Materials: The following supporting information can be downloaded at: <https://www.mdpi.com/article/10.3390/liquids4020016/s1>; Figure S1: Some stationary point (non-minimum) energy structures of aquaantimony(III); Table S1: Total Energies of Aquaantimony(III) Species.

Author Contributions: Conceptualization, C.C.P.; methodology, C.C.P.; validation, C.C.P.; formal analysis, C.C.P.; investigation, C.C.P. and C.M.G.; data curation, C.C.P.; writing—original draft preparation, C.C.P.; writing—review and editing, C.C.P.; visualization, C.C.P. and C.M.G.; supervision, C.C.P.; project administration, C.C.P.; funding acquisition, C.C.P. All authors have read and agreed to the published version of the manuscript.

Funding: This research was funded by the Natural Sciences and Engineering Research Council of Canada and the Department of Economic Development, Government of Nova Scotia.

Data Availability Statement: The data presented in this study are available in the Supplementary Materials.

Acknowledgments: The authors thank the Department of Astronomy and Physics, Saint Mary's University (AP-SMU), for providing access to computing facilities, in particular, to cygnus, a 10-processor Sun server, purchased with assistance from the Canada Foundation for Innovation, Sun Microsystems, the Atlantic Canada Opportunities Agency, and SMU. C.C.P. also thanks ACEnet and Compute Canada for providing access to computers and Gaussian 03/16. C.C.P. acknowledges the former financial support of NSERC. C.M.G. acknowledges the support of the Department of Economic Development (Government of Nova Scotia), the Office of the Dean of Science, SMU, and the Cooperative Education program (SMU—Work Term 2, Fall 2001 and Work Term 3, Winter 2002).

Conflicts of Interest: The authors declare no conflicts of interest. The funders had no role in the design of the study; in the collection, analyses, or interpretation of data; in the writing of the manuscript; or in the decision to publish the results.

References

1. Richens, D.T. *The Chemistry of Aqua Ions*; Wiley: Chichester, UK, 1997.
2. Pye, C.C.; Gunasekara, C.M. An Ab Initio Investigation of the Hydration of Thallium(III) and Mercury(II). *J. Solut. Chem.* **2020**, *49*, 1419–1429. [[CrossRef](#)]
3. Pye, C.C.; Gunasekara, C.M. An Ab Initio Investigation of the Hydration of Lead(II). *Liquids* **2022**, *2*, 39–49. [[CrossRef](#)]
4. Pye, C.C.; Gunasekara, C.M. An Ab Initio Investigation of the Hydration of Tin(II). *Liquids* **2022**, *2*, 465–473. [[CrossRef](#)]
5. Gayer, K.H.; Garrett, A.B. The Equilibria of Antimonous Oxide (Rhombic) in Dilute Solutions of Hydrochloric Acid and Sodium Hydroxide at 25°. *J. Am. Chem. Soc.* **1952**, *74*, 2353–2354. [[CrossRef](#)]
6. Mishra, S.K.; Gupta, Y.K. Spectrophotometric Study of the Hydrolytic Equilibrium of Sb(III) in Aqueous Perchloric Acid Solution. *Ind. J. Chem.* **1968**, *6*, 757–758.
7. Baes, C.F., Jr.; Mesmer, R.E. *The Hydrolysis of Cations*; Wiley: New York, NY, USA, 1976.
8. Ahrlund, S.; Bovin, J.-O. The Complex Formation of Antimony(III) in Perchloric Acid and Nitric Acid Solutions. A Solubility Study. *Acta Chem. Scand. A* **1974**, *28*, 1089–1100. [[CrossRef](#)]
9. Zakaznova-Herzog, V.P.; Seward, T.M. Antimonous acid protonation/deprotonation equilibria in hydrothermal solutions to 300 °C. *Geochim. Cosmochim. Acta* **2006**, *70*, 2298–2310. [[CrossRef](#)]
10. Natta, G.; Baccaredda, M. Composti chimici interstiziali. Struttura del pentossido di antimonio idrato e di alcuni antimoniati. [Interstitial chemical compounds. Structure of hydrated antimony pentoxide and some antimonates]. *Gazz. Chim. Ital.* **1936**, *66*, 308–316. (In Italian)
11. Dihlstrom, K.; Westgren, A. Uber den Bau des sogenannten Antimontetroxyds und der damit isomorphen Verbindung $\text{BiTa}_2\text{O}_6\text{F}$. [About the construction of the so-called antimony tetroxide and the isomorphous compound $\text{BiTa}_2\text{O}_6\text{F}$]. *Z. Anorg. Allg. Chem.* **1937**, *235*, 153–160. (In German) [[CrossRef](#)]
12. England, W.A.; Cross, M.G.; Hamnett, A.; Wiseman, P.J.; Goodenough, J.B. Fast Proton Conduction in Inorganic Ion-Exchange Compounds. *Solid State Ion.* **1980**, *1*, 231–249. [[CrossRef](#)]

13. Watelet, H.; Picard, J.-P.; Baud, G.; Besse, J.-P. Chevalier, R. Un nouveau conducteur protonique, $[H(H_2O)_n]_{12}Sb_{12}O_{36}$ ($n \leq 1$). [A new protonic conductor, $[H(H_2O)_n]_{12}Sb_{12}O_{36}$ ($n \leq 1$).] *Mater. Res. Bull.* **1981**, *16*, 1131–1137. (In French) [[CrossRef](#)]
14. Jager, G.; Jones, P.G.; Sheldrick, G.M.; Schwarzmann, F. Darstellung und Kristallstruktur von Antimonen(V)oxidhydroxid HSb_3O_8 . [Representation and Crystal Structure of Antimony(V) Oxide Hydroxide HSb_3O_8 .] *Z. Naturforschung B* **1983**, *38*, 698–701. (In German) [[CrossRef](#)]
15. Riviere, M.; Fourquet, J.L.; Grins, J.; Nygren, M. The cubic pyrochlores $H_{2x}Sb_{2x}W_{2-2x}O_6 \cdot nH_2O$: Structural, thermal, and electrical properties. *Mater. Res. Bull.* **1988**, *23*, 965–975. [[CrossRef](#)]
16. Svensson, C. Refinement of the Crystal Structure of Cubic Antimony Trioxide, Sb_2O_3 . *Acta Cryst. B* **1975**, *31*, 2016–2018. [[CrossRef](#)]
17. Svensson, C. The Crystal Structure of Orthorhombic Antimony Trioxide, Sb_2O_3 . *Acta Cryst. B* **1974**, *30*, 458–461. [[CrossRef](#)]
18. Orosel, D.; Dinnebier, R.E.; Blatov, V.A.; Jansen, M. Structure of a new high-pressure-high-temperature modification of antimony(III) oxide, γ - Sb_2O_3 , from high-resolution synchrotron powder diffraction data. *Acta Crystallogr. B* **2012**, *68*, 1–7. [[CrossRef](#)] [[PubMed](#)]
19. Bovin, J.P. The crystal structure of $Sb_4O_4(OH)_2(NO_3)_2$. *Acta Chem. Scand. A* **1974**, *28*, 267–274. [[CrossRef](#)]
20. Bovin, J.P. The crystal structure of $Sb_4O_5(OH)ClO_4 \cdot 1/2 H_2O$. *Acta Chem. Scand. A* **1974**, *28*, 723–730. [[CrossRef](#)]
21. Bovin, J.P. The Crystal Structure of the Antimony(III) Oxide Sulphate $Sb_6O_7(SO_4)_2$. *Acta Cryst. B* **1976**, *32*, 1771–1777. [[CrossRef](#)]
22. Mercier, R.; Douglade, J.; Jones, P.G.; Sheldrick, G.M. Structure of an Oxonium Antimony(III) Sulphate, $(H_3O)_2Sb_2(SO_4)_4$. *Acta Cryst. C* **1983**, *39*, 145–148. [[CrossRef](#)]
23. Frisch, M.J.; Trucks, G.W.; Schlegel, H.B.; Scuseria, G.E.; Robb, M.A.; Cheeseman, J.R.; Zakrzewski, V.G.; Montgomery, J.A., Jr.; Stratmann, R.E.; Burant, J.C.; et al. *Gaussian 98, Revision A.9*; Gaussian, Inc.: Pittsburgh, PA, USA, 1998.
24. Frisch, M.J.; Trucks, G.W.; Schlegel, H.B.; Scuseria, G.E.; Robb, M.A.; Cheeseman, J.R.; Montgomery, J.A., Jr.; Vreven, T.; Kudin, K.N.; Burant, J.C.; et al. *Gaussian 03, Revision D.02*; Gaussian, Inc.: Wallingford, CT, USA, 2004.
25. Frisch, M.J.; Trucks, G.W.; Schlegel, H.B.; Scuseria, G.E.; Robb, M.A.; Cheeseman, J.R.; Scalmani, G.; Barone, V.; Petersson, G.A.; Nakatsuji, H.; et al. *Gaussian 16, Revision A.03*; Gaussian, Inc.: Wallingford, CT, USA, 2016.
26. Pye, C.C.; Gunasekara, C.M.; Rudolph, W.W. An ab initio investigation of bismuth hydration. *Can. J. Chem.* **2007**, *85*, 945–950. [[CrossRef](#)]
27. Pye, C.C.; Whynot, D.C.M.; Corbeil, C.R.; Mercer, D.J. Desymmetrization in geometry optimization: Application to an ab initio study of copper(I) hydration. *Pure Appl. Chem.* **2020**, *92*, 1643–1654. [[CrossRef](#)]
28. Pye, C.C.; Gilbert, C.R. An ab initio investigation of the second hydration shell of metal cations. *Comput. Appl. Chem.* **2020**, *37*, 2020. [[CrossRef](#)]
29. Shimony-Livny, L.; Glusker, J.P.; Bock, C.W. Lone Pair Functionality in Divalent Lead Compounds. *Inorg. Chem.* **1998**, *37*, 1853–1867. [[CrossRef](#)]

Disclaimer/Publisher’s Note: The statements, opinions and data contained in all publications are solely those of the individual author(s) and contributor(s) and not of MDPI and/or the editor(s). MDPI and/or the editor(s) disclaim responsibility for any injury to people or property resulting from any ideas, methods, instructions or products referred to in the content.